We are IntechOpen,
the world's leading publisher of
Open Access books
Built by scientists, for scientists

6,900
Open access books available

185,000
International authors and editors

200M
Downloads

154
Countries delivered to

Our authors are among the

TOP 1%
most cited scientists

12.2%
Contributors from top 500 universities

BOOK CITATION INDEX
CLARIVATE ANALYTICS
INDEXED

WEB OF SCIENCE™

Selection of our books indexed in the Book Citation Index
in Web of Science™ Core Collection (BKCI)

Interested in publishing with us?
Contact book.department@intechopen.com

Tribocorrosion: Material Behavior Under Combined Conditions of Corrosion and Mechanical Loading

Pierre Ponthiaux[1], François Wenger[1] and Jean-Pierre Celis[2]
[1]Ecole Centrale Paris, Dept. LGPM, Châtenay-Malabry,
[2]Katholieke Universiteit Leuven, Dept. MTM, Leuven,
[1]France
[2]Belgium

1. Introduction

1.1 Definition of tribocorrosion

Tribocorrosion can be defined as the study of the influence of environmental factors (chemical and/or electrochemical) on the tribological behavior of surfaces. In other words, the process leading to the degradation of a metallic and/or non-metallic material resulting from a mechanical contact (sliding, friction, impact, ...) combined to a corrosive action of the surrounding environment.

The origin of tribocorrosion is closely related to the presence of a passive film on material surfaces subject to wear and the modifications of these surfaces by friction or any other form of mechanical loading. In very general terms, the passive film (mainly oxide) is considered to be snatched in the contact area.

Oxide particles, referred to as 'debris", are released from the contacting materials. Then, the debris can be removed from the contact zone or on the contrary trapped in it. In the case of removal, the debris dissolve chemically or are dragged out by a hydraulic flow along the material surface. In this case, the tribocorrosion mechanism is based on a repeated tearing off of the oxide after each contact and eventually a removal of some of the underlying material depending on the intensity of mechanical stress acting on the contacting materials. The major concern is then to quantify and eventually to model the kinetics of repassivation as accurately as possible. This type of tribocorrosion process can be classified as an oxidative wear mechanism as, for example, the 'mild oxidative wear model' (Quinn, 1992). In the case of debris trapping, one has to consider that under appropriate hydrodynamical, chemical, and thermal contact conditions and relative speed of the two contacting bodies, the debris will remain temporarily in the contact zone mainly as colloids with a diameter usually in the range of a few hundred nanometers. Two cases may then be distinguished: (a) the debris accelerates the wear in comparison to the case of debris-free contacts is accelerated by an abrasive effect, or (b) the debris slows down the wear compared to the case where the contact zone is free of any debris, resulting in a protective effect.

Tribocorrosion may take place in practice in a large number of very different tribological systems consisting of mechanical devices containing metallic parts that are in contact with counterparts and exhibiting a relative movement placed in an environment revealing itself to be corrosive to at least one of the contacting materials. A non-limitative list of examples might contain machinery pumps, bearings, gears, ropes, electrical connectors, hinges, microelectromechanical systems (MEMs), and orthopedic implants like hip and knee implants.

1.2 Synergism between mechanical and chemical loading

To understand the importance and complexity of the phenomena taking place under tribocorrosion, one has to consider that the corrosiveness of a medium (liquid or gas) towards a material is highly dependent on the mechanical stresses that act onto a material, particularly at its surface exposed to that environment.

In tribocorrosion, five mechanisms may explain the synergism noticed between mechanical and chemical factors acting on contacting materials, namely:

1. the debris can speed up or reduce wear compared to what happens in the same environment where debris does not exist like e.g. in sliding contacts polarized at a large cathodic potential,
2. a galvanic coupling is established between the worn and unworn areas. It accelerates the anodic dissolution in the area where the metal is depassivated,
3. a galvanic coupling may be established between the two contacting counterparts,
4. an accumulation of dissolved species may take place in the liquid surrounding the contact. This may render the medium chemically or electrochemically more aggressive,
5. the mechanical loading in the contact area and its nearby zone may causes a work hardening of the materials. This work hardening can alter the kinetics of corrosion and/or repassivation processes.

A synergistic effect occurs in tribocorrosion when the mechanical process affects the corrosion process acting in a tribological system or vice versa. In these cases, the wear, W, found on a given component in a tribological system subjected to a mechanical loading in a given corrosive environment, will be very different and often much greater than the sum of the mechanical wear, W_{mo}, measured as a material loss under a given mechanical load in the absence of a corrosive environment, and the material loss induced by corrosion, W_{co}, in the absence of any mechanical contact (see Equation 1):

$$W \neq W_{mo} + W_{co} \tag{1}$$

This result is partly explained by the fact that the corrosion resistance in the case of a metal depends on the presence at its surface of reaction layers, sometimes only a few atom layers thick, resulting from an interaction between the material and the surrounding environment. Such layers can be classified as oxides, solid precipitates, adsorbed layers, or passive surface films. Some of them like dense oxide layers, precipitates, or passive films play a protective role by isolating the underlying metal from a direct contact with a surrounding corrosive environment. This is particularly true in the case of stainless steels and other alloys containing chromium. Their passive surface film formed in ambient air or in contact with an

aqueous solution is a few nanometers thick but gives them a high resistance to corrosion. The sliding of a hard counterbody material on such a surface is likely to damage that passive film what is known as a "depassivation" process by which the bare material is exposed to the corrosive environment. Various but essentially electrochemical processes can then compete on these bare surfaces, namely:

- the dissolution of the metal in the corrosive medium,
- the formation of a new compound that may contribute to the breakdown process, and
- the restoration of the protective film known as "repassivation" process.

1.3 Complexity of the tribocorrosion process

The following examples taken from literature illustrate quite well the numerous parameters and interactions that govern the tribocorrosion process. Lemaire & Le Calvar, 2000, described the wear of a cobalt-based alloy coating generally referred to as "stellite 6" applied on the gripper latch arms of the control rods command mechanisms in pressurized water reactors (PWR). The downwards movement of the control rods is controlled by gripper latch arms of which the protruding teeth are coated with Stellite 6. The teeth block the movement once they come in contact with the control bar at the circular grooves lining their surface. At each blocking step, there is a contact between teeth and inner part of the grooves at a moderate pressure estimated at 150 MPa. Subsequently a sliding takes place over a distance of approximately 0.1 mm before the control rods come to rest. In the middle of the primary cooling circuit stellite 6 does not undergo any significant corrosion in the absence of any mechanical stress, thanks to the protective action of the passive film on stellite 6 consisting of chromium oxides. However under field operating conditions where impact and sliding of the teeth on the control bar take place, corrosion is evident. The wear observed on the teeth was found not to depend only on the number of blocking steps as would be the case in absence of corrosion. But the wear was found to depend also on the time interval between two successive blocking steps. The wear rate for a given number of blocking steps appeared to increase with the latter.

A plausible hypothesis to interpret this behavior is to consider that between two successive blocking steps corrosion takes place on parts of the surface where the passive film was mechanically damaged in the preceding step. The wear progress is correlated with the time interval between successive blocking steps by the following simple empirical equation (Bom Soon Lee et al., 1999):

$$I(t) = I_0 \left(\frac{t}{t_0} \right)^{-n} + I_p \tag{2}$$

in which I(t) is the evolution of the dissolution current of a metal with time starting at the time the metal becomes depassivated due to a mechanical action and extending during the film restoration where dissolution and repassivation are competitive surface processes. The parameters I_0 and t_0 are constants, while I_p is the passivation current under steady state, and n has a value between 0.3 and 1.

However, the effect of sliding on the electrochemical reactivity of the surface of a metal is not always confined to the partial destruction of surface layers. Other phenomena resulting directly or indirectly from contacts between parts can influence the corrosion behavior of their surfaces. For example, under reciprocating sliding conditions at small displacement amplitude, known as fretting (Carton et al., 1995; Godet et al, 1991) cracks may appear at the rim of the contact zone even after only a small number of contact events. Another parameter to be considered in tribocorrosion is the stirring of the corrosive environment along the surfaces of contacting parts caused by their relative movement. It affects tribocorrosion since such a stirring modifies the transport kinetics of chemical species that are generated in the vicinity of the surfaces due to the corrosion-related reactions.

The effect of the environment (mechanical or physico-chemical) on the crack propagation is evident. This returns us, somehow, to the notion of stress corrosion with the nuance that the cracks are induced at a mechanical loading which is not constant in the fretting test under consideration.

In addition one has to consider the possible role of strain hardening and/or structural transformations induced by the sliding action on the electrochemical reactivity of the surface, speeding up or slowing down some reactions. The resulting material transformation may end up in the most stable phase of the material considered being a supersaturated solid solution obtained by the gradual dissolution of pre-existing precipitates. It may also become a nano-crystalline network of a few tens of nanometers in average size that contains a high density of dislocations with no preferred orientation. This structure is very hard but also very fragile. Its intrinsic reactivity with the environment differs necessarily from the one of the original surface. Moreover, starting with the formation of a network of micro-cracks on it, wear particles (known as 'debris') are generated.

In the case of tribocorrosion, it is important to consider the galvanic coupling that might result from the heterogeneity of the electrochemical state of non-rubbed surfaces, and rubbed surfaces undergoing a strain hardening and on which the surface layers are altered. This galvanic coupling causes the polarization of non-rubbed and rubbed areas, and modifies the kinetics of reactions in these areas.

One has also to consider the existence of a third body that consists of wear particles as visible in Figure 1. At first, this third body may interact with the environment to form oxides or hydroxides. If they are ejected out of the contact zone, they become strictly speaking 'debris' and contribute to a material loss. If they remain in the contact zone, they can modify the mechanical response of the system by favoring a sliding action between counterparts, by acting as an abrasive agent promoting the so-called "abrasive wear", or by affecting the reactivity of material surfaces.

In return, a corrosion process can modify the surface states of materials and in consequence the contact conditions. In that way corrosion can affect the sliding conditions (coefficient of friction, wear regime, ...). The interaction between friction and corrosion therefore induces a complex phenomenon of synergy.
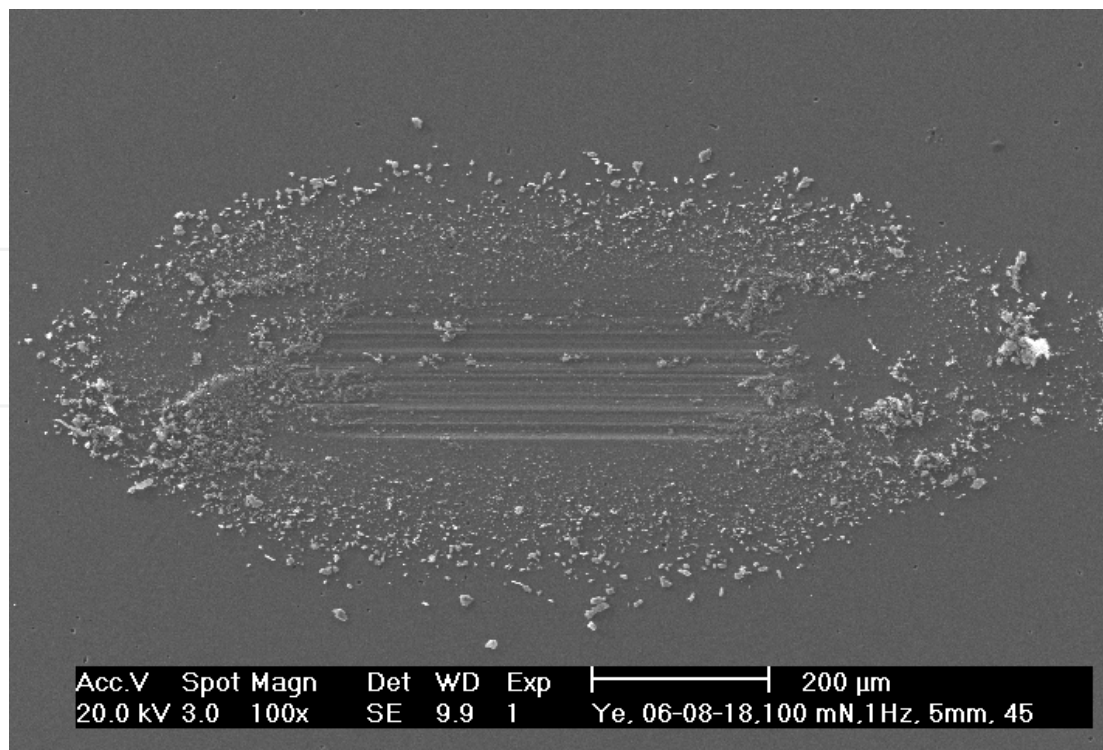
Fig. 1. Example of a third body resulting from a tribological process during reciprocating sliding. Some abrasive grooves are also visible in the central area of the sliding track.

2. The *in situ* study of tribocorrosion processes by electrochemical techniques

When performing a tribocorrosion test, one has to implement not only the following traditional concepts of tribological testing, namely:

- the representativeness of the contact (e.g. sphere-on-flat, sphere, cylinder-on-flat, flat-on-flat,...),
- the choice of the type of relative movement (continuous or reciprocating),
- the applied forces and the relative velocities, accelerations or displacements,
- the influence of the characteristics of the tribometer used on the wear induced, and
- the similarity of the wear mechanisms active in the laboratory test and in the field,

but he has also to take into account and to control simultaneously a large number of testing parameters, like:

- mechanical ones (e.g. contact frequency, noise, vibrations, surface roughness and residual stress ...),
- metallurgical ones (e.g. composition and structural state of contacting materials, microstructure, surface film composition and structure ...), and
- environmental ones (e.g. composition of the corrosive environment, pH, aggressiveness, viscosity, ionic conductivity, temperature, solid particles in suspension, stagnant or stirred,..).

These parameters determine the electrochemical reactivity of the surfaces and in consequence influence the contact conditions (wear regime, existence of a third body, friction ...).

Such tests therefore need to be instrumented to control and/or to record the contact conditions like the normal or tangential force, the relative displacement, velocity, acceleration and contact frequency ...). They need also to be instrumented with electrochemical techniques enabling the control and/or the recording of electrochemical parameters like the polarization of the contacting materials.

The choice of electrochemical techniques that can be implemented in a tribocorrosion test and the development of relevant models for the interpretation of the tribocorrosion mechanism are determined by the mechanical contact conditions being continuous or reciprocating. Electrochemical measurements can be performed with both types of tribometers. However, to be implemented under conditions that allow the interpretation of results, some methods require stationary electrochemical conditions, at least prior to starting up the measurements. In the case of continuous sliding, a quasi-stationary electrochemical surface state can often be reached, and all the electrochemical techniques available for corrosion studies (polarization curves, impedance spectroscopy, electrochemical noise,...), can be used. On the contrary, when reciprocating contact conditions prevail, the interpretations of experimental results are more complex due to the non-stationary electrochemical conditions. Measuring techniques suitable for the recording of current or potential transients will be used preferentially (Mischler et al., 1997; Rosset, 1999).

2.1 Open circuit potential measurements

Under sliding conditions, the measured open circuit potential is a mean value which depends on the electromotive force induced by the surface heterogeneity resulting from the coexistence of non-rubbed and rubbed areas which are in different electrochemical states, and on the areas of these zones and their spatial distribution that determines the non-uniform distribution of potential over the whole surface (Oltra et al, 1986). When applying for example a continuous sliding, this open circuit potential responds to the mechanical loading imposed, as shown in Table 1 and Figure 2.

Fn (N)	0	2.2	2.2	4.2
V (cm s-1)	0	0.5	0.8	0.8
Eoc (V vs SCE)	-0.15	-0.29	-0.32	-0.42

Table 1. Variations of the open-circuit potential E_{OC} of 316L stainless steel in artificial sea water as a function of varying tribological contact conditions. S.C.E.: saturated calomel electrode. F_n: normal force. V: sliding speed.
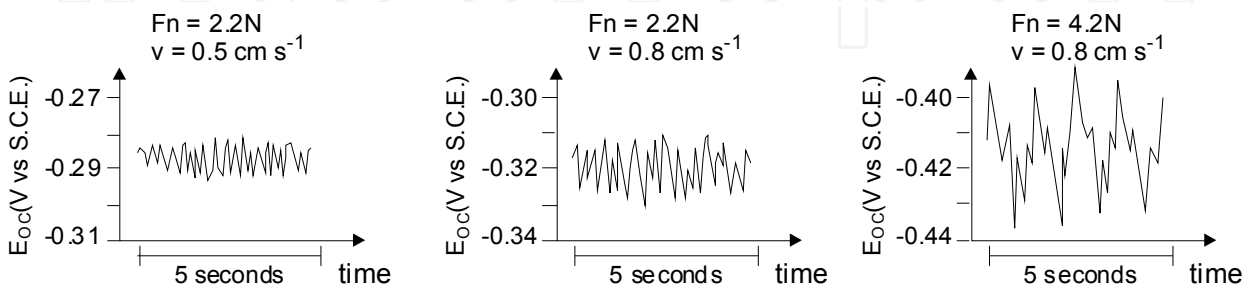

Fig. 2. Electrochemical noise at the open circuit potential E_{OC} of 316L stainless steel in artificial sea water for different tribological contact conditions. S.C.E.: saturated calomel electrode. F_n: normal force. V: sliding speed.

Table 1 gives the evolution of the mean value of the open circuit potential of a 316 L stainless steel in contact with alumina immersed in artificial seawater for different normal forces and velocities (Ponthiaux et al., 1997). Alumina is taken since it has a high electrical resistance and is chemically inert in the liquid used. At a zero normal force and speed, the measured open circuit potential corresponds to the passive state of the entire stainless steel surface. When the normal force or the speed increases, the open circuit potential shifts towards lower potential values. This shift can be explained by considering the following phenomena:

- on the rubbed area, the surface layer on materials can be partially destroyed (also called "depassivation") and that rubbed area acquires a potential that corresponds to the one of an "active material" undergoing dissolution or on which reduction reactions can take place, and
- an increase of the normal force or velocity tends to increase the area of active material.

In Figure 2, the rapid fluctuations of the open circuit potential arising during sliding are represented schematically. They constitute an 'electrochemical noise' representing the electrochemical response to the rapid and stochastic fluctuations of the new bare metal surface generated in the real contact area by sliding friction. This noise can provide information on the mechanism of friction as well as on the mechanism of electrochemical reactions involved in the depassivation – repassivation process (Déforge et al.). A more detailed analysis of open circuit potential measurements under sliding requires a more precise knowledge of the local surface state of contacting materials. Experimentally, microelectrodes can be used to determine potential values of rubbed and non-rubbed areas. Such techniques have already been used to study localized corrosion, and models have been proposed (Lillard et al., 1995). Note that the interpretation of local potential measurements or the development of theoretical models describing the potential distribution, can only be obtained with realistic assumptions on the reaction kinetics of reactions occurring at rubbed and non-rubbed surface areas. Such Information can only be obtained by using complementary methods.

2.2 Potentiodynamic polarization measurements

Potentiodynamic polarization curves obtained at increasing and decreasing potential scan in absence of any sliding is schematically shown in Figure 3. In the case the current measured originates from the whole surface of the tested sample that might be considered as being uniform.

Under sliding conditions, the currents measured during potentiodynamic polarization are in a first approach the sum of two components, namely the current originating from the rubbed area, and the one linked to the non-rubbed area. Under such conditions, the maximum dissolution current, I_M, varies with the mean contact pressure and sliding speed. However, these two test parameters do not necessarily affect in the same way the electrochemical behavior of the alloy:

- at constant speed an increase of the mean contact pressure may cause a decrease of the maximum dissolution current, I_M. This reflects then a slowing down of the dissolution of the alloy which can be due to the strain hardening of the material in the rubbed area. Moreover, the potential, E_M, at which this maximum current is noticed, remains almost

unaffected. This indicates that the dissolution process is the same on rubbed and non-rubbed materials,

- at a fixed mean pressure, an increase of the sliding speed may cause, in turn, an increase of the maximum dissolution current. This increase of I_M is then a consequence of the increased bare surface area generated per unit of time. It indicates in that case that the dissolution of the bare material is faster than the non-rubbed material.
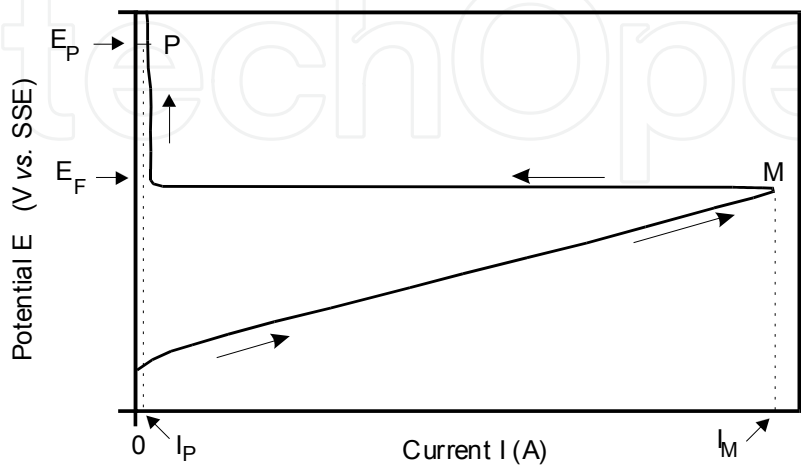

Fig. 3. Schematic potentiodynamic polarization curve recorded on a passivating metallic material (Fe-30%Ni alloy) in absence of any sliding: E_F = Flade potential, E_M = potential at maximum dissolution current I_M, I_P = passivation current.

The possible evolution of the passivation current, Ip, under sliding friction with the mean contact pressure, P_M, and the sliding velocity is schematically shown in Figure 4. That passivation current is increasing with these two testing parameters. That increase can be related to an increase in bare surface area due to:

- an increasing contact area with increasing normal force, and
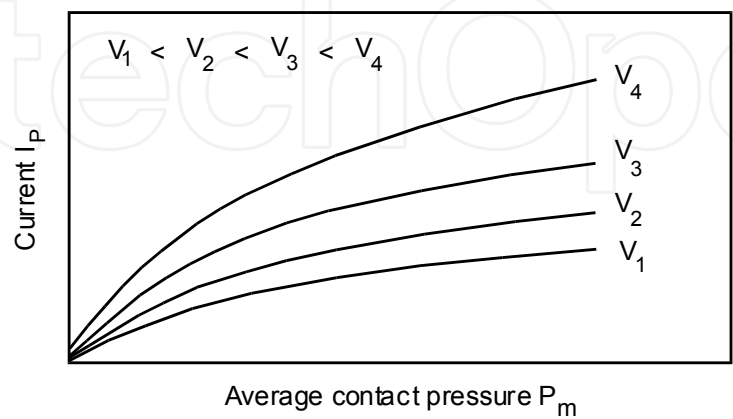- an increasing depassivated surface area generated per unit time with increasing sliding speed.

Fig. 4. Evolution of the passive current, I_p, with the mean contact pressure, P_m, at increasing sliding speeds. Example of a Fe-31%Ni alloy disc immersed in 0.5 M sulfuric acid and polarized at a fixed passive potential, under continuous sliding against alumina.

The extent of the passivation range is in general affected by the sliding. In some cases the Flade potential, E_F, shifts towards more anodic values at increasing contact pressure. This means that the stability of the passive film decreases. When the potential E_F is reached, the entire surface becomes active and dissolves. However, under these experimental conditions, the disruption of the passive film is only a local disturbance in the sliding track in a relatively small area that represents generally not more than 10% of the total sample area. Therefore sliding does not only affect the electrochemical state of the rubbed surface, but also the state of the whole surrounding sample surface.

Finally it should be stressed that the coefficient of friction varies with the applied potential during a potentiodynamic polarization. Changes in the value of the coefficient of friction reveal a possible change in the surface state of the materials in the sliding track (Ponthiaux et al., 1999).

The in-depth interpretation of the polarization curves frequently faces difficulties related to the non-uniform distributions of current and potential on the sample surface. This non-uniformity originates from the intrinsic effect of the sliding that causes an heterogeneity of the electrochemical surface reactivity, combined with the ohmic drop in the electrolyte. A full exploitation of the polarization curves in terms of local behavior is possible only if one can model the current and potential distributions under sliding conditions. This brings back to the same approach as in the case of the interpretation of open circuit potential measurements. Note that the effect of non-uniform distributions on the interpretation of polarization curves was already investigated in the absence of any sliding (Law & Newman, 1979; Ponthiaux et al., 1995; Tiedemann et al., 1973).

2.3 Repassivation current transients

Methods based on analysis of potential or current transients (Ponthiaux et al., 1995) are particularly well suited to study reciprocating sliding tests (Mischler et al., 1997). These methods are used to study between successive contact events, the rebuild of damaged surface layers (oxide, passive film ...). Under imposed polarization e.g. in the passivation range, at each stop-start event, a transient variation of current is noticed with time (see Figure 5). The charge corresponding to this transition can be attributed to the re-growth of a uniform film in the damaged area.
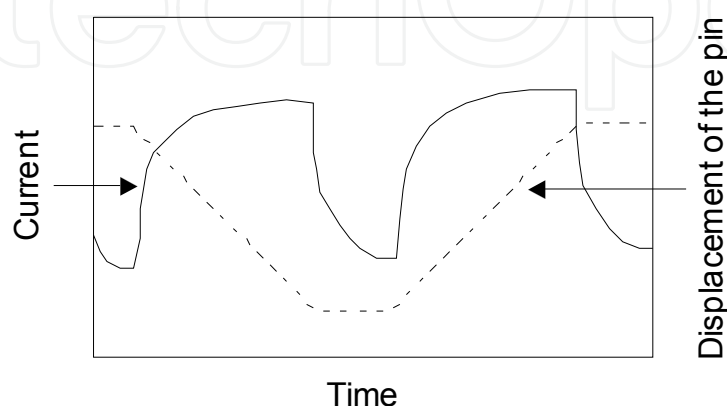

Fig. 5. Schematic evolution of the current transients obtained under reciprocating sliding.

In order to study in more details the mechanism and kinetics of a re-growth of the passive film, the "potential jump" method can be used. However, such a method cannot be applied on metals such as aluminum, for which the passive film can not be reduced by a cathodic polarization, or for some steels for which the contamination of the surface by reduction products can affect the initial current increase at the potential jump.

2.4 Electrochemical impedance measurements

This method requires quasi-stationary electrochemical conditions of currents and potentials. The impedance measurements allow the study of the influence of sliding on the elementary processes involved in the corrosion mechanism. By performing a systematic analysis of the changes in the impedance diagrams with the sliding parameters like normal force and sliding speed or contact frequency, a model can be developed incorporating the sliding effects in the mechanism.

Impedance measurements recorded on a non-rubbed and a rubbed Fe-31% nickel alloy are shown in Figure 6. The measurements were done in 0.5 M sulfuric acid at a potential of -675 mV / SSE located in the active region (Boutard et al., 1985). The impedance diagrams were recorded in a limited range of measurement frequencies. In particular, under sliding, the impedance was not measured at frequencies below 0.01 Hz, to limit the duration of the measurements and to avoid in this way the influence of the long-term evolution of the electrochemical state of the surface due to wear - induced changes in the "rubbed area/unrubbed area" ratio. By taking these precautions, we can consider that the condition of average electrochemical steady-state required for impedance measurements is fulfilled.
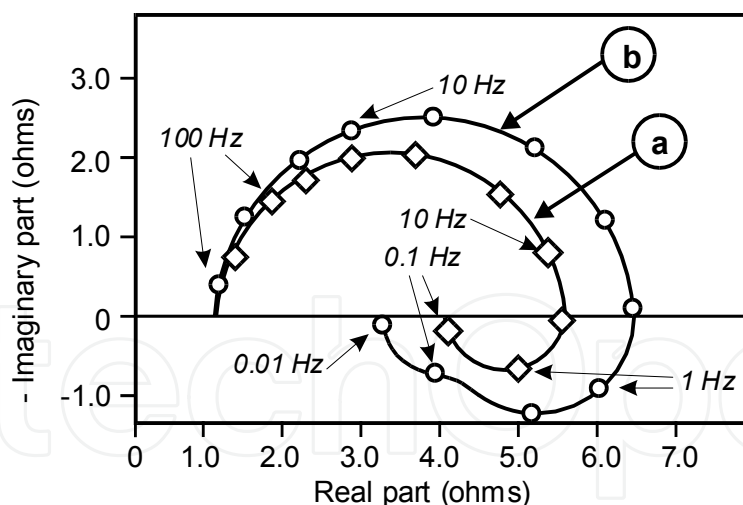

Fig. 6. Electrochemical impedance plots recorded on Fe-31% Ni immersed in 0.5 M sulfuric acid polarized in the active region (-0,675 V/SSE): (a) in absence of any sliding, and (b) under continuous sliding against alumina at a mean contact pressure of 2,6 MPa and a sliding speed of 3,4 cm s^{-1} (Ponthiaux et al., 1999).
SSE: 'mercury/mercurous sulfate/saturated potassium sulfate' reference electrode
(E_{SSE} = +0.65 V/NHE).

In absence of friction, the plot consists of two successive semi-circles, a capacitive one reflecting the dielectric properties of the electrochemical double layer, and an inductive one

reflecting the contribution of an elementary adsorption step in the reaction mechanism. Under sliding, the shape and size of the plot are modified as follows:

- at high frequencies, the capacitive arc increases reflecting a lower dissolution rate. This might be correlated to a strain hardening effect mentioned above, and highlighted in the polarization curves, and
- at low frequencies, an additional inductive arc appears which highlights the presence of a second adsorbate in the dissolution mechanism.

This can be interpreted by considering that in a non-rubbed condition the semi-circle linked to a possible second adsorbate does not appear because its concentration at the surface of the sample does not vary substantially with the potential. Under sliding conditions, the kinetics of some dissolution steps evolves, in particular the kinetics of steps in which the adsorbate interacts. The variation of the concentration at the surface becomes then detectable.

The in-depth interpretation of these impedance diagrams encounters however some difficulties as those already reported for open circuit potential and polarization measurements which are related to the heterogeneous state of the tested surfaces.

A first difficulty results from the fact that the impedance data reflect the overall state of the tested surface integrating the contributions of non-rubbed and rubbed surfaces. Such data must thus be de-convoluted in order to obtain the specific impedances of these two types of surface states. A first approach to this problem might be to use models similar to those describing the impedance of a sample undergoing a localized corrosion (Oltra & Keddam, 1990). In that specific case, the overall impedance can be considered as the result of two impedances in parallel, namely the impedance of the non-rubbed surface and the one of the rubbed surface. A strict interpretation requires further an evaluation of the areas of these surfaces, e.g. by using profilometry and surface observations by light optical or scanning electron microscopy.

The second difficulty results from the non-uniform state of the rubbed surface. Behind the slider the sample surface can be laid bare for some time before some new surface layers are rebuilt. The restored surface increases gradually with the distance behind the slider along the sliding track. Even if the first difficulty was already solved and the overall impedance of the rubbed surface is obtained, it can not be used as such to characterize the non-uniform distribution of the electrochemical states behind the slider. However, it is expected that impedance measurement procedures already developed for analyzing non-uniform distributions of surface states and the electrochemical models developed for the interpretation of such measurements (Zhang et al., 1987) could be transferred to tribocorrrosion test conditions. Such a study could allow a localized characterization of dissolution and passivation kinetics.

If theoretically this approach seems promising, experimental data analyses show that impedance measurements under sliding are often disturbed at low frequencies due to the random fluctuations of potential or current. This "electrochemical noise" limits unfortunately to some extent the application of impedance measurements. Limitations frequently originate from the sliding action itself and more specifically from the localized damages induced in the contact area by the mechanical interaction. Notwithstanding that, the in-depth analysis of the electrochemical noise will surely in the future be fruitful since it will contain useful information on the progress of the process at both spatial and time scales.

2.5 Electrochemical noise analyses

In the case of tribocorrosion as in cases involving stochastic processes of local surface damages like pitting (Uruchurtu & Dawson, 1987), stress corrosion (Cottis & Loto, 1990), and corrosion-abrasion (Oltra et al., 1986), sliding destroys locally to some extent surface layers. The bare areas created by the slider generate fluctuations of potential or current which consist of the superposition of elementary transients. The sudden increase in current occurs at the time that a bare surface is brought in contact with the electrolyte. The subsequent current decrease reveals the restoration of a protective surface film. The analysis of the transient characteristics (shape, amplitude, duration) provides information on the mechanisms and kinetics of the reactions involved (e.g. dissolution, passivation). The frequency of the transients depends in turn on the number of contacting points in the sliding track at a given time and on the sliding rate of the slider. It is therefore a quantity that provides useful information on the nature of the contact.

Sliding conditions affect the amplitude of the electrochemical noise, namely fluctuations of the open circuit potential as shown in Figure 2 (Ponthiaux et al., 1997). It is usually impossible to isolate the elementary transients. However, the spectral analysis of such a noise allows characteristic quantities to be derived such as the mean amplitude or duration and the average frequency at which transients occur. These characteristics are essential for getting a better understanding of the nature of the contact and the dissolution and passivation kinetics on the bare surface.

3. Modeling approaches

Given the complexity of the tribocorrosion phenomena there is currently no universal predictive model of the wear-corrosion process available. Such a problem solving is largely empirical, and designers rely on expert systems fed by experimental feedback to select the material couples for a given tribological system. In parallel to this technical approach, scientists are developing the modeling elements needed to unravel the phenomena. These models are discussed hereafter.

3.1 Formalism of the wear-corrosion synergy

It was shown here above that electrochemical methods allow under certain conditions to measure in real time the current I related to the corrosion reaction in a sliding track. At the end of a tribocorrosion experiment (e.g. sliding or erosion tests), the electrochemical mass loss, C, can be calculated using Faraday's relationship from the total charge consumed by the corrosion process:

$$C = \frac{M}{nF}Q \qquad (3)$$

in which M is the atomic mass of the metal, n is the valency of the oxidized metal in the environment studied, F is the Faraday's constant and Q is the total charge related to the corrosion process, namely

$$Q = \int_0^T I(t)\,dt$$

with T the total duration of the test. However, the electrochemical mass loss due to corrosion under sliding, C, is generally not equal to the mass loss of the metal, C_0, obtained under similar test conditions but in absence of any sliding. The electrochemical mass loss under sliding C has thus to be expressed as:

$$C = C_0 + C_M \tag{4}$$

with C_M the amount of corrosion induced by wear.

The total mass loss, *W*, can be determined at the end of a sliding test by some *ex situ* technique like surface profilometry or gravimetry. That total mass loss can be compared to the electrochemical mass loss under sliding, *C*, from the equation:

$$W = C + M \tag{5}$$

in which M is the mechanical mass loss. This mechanical mass loss M can also be compared to the mass loss, M_0, in a non-corrosive environment as:

$$M = M_0 + M_C \tag{6}$$

in which M_C represents the excess mechanical mass loss due to corrosion. This formalism now allows a general definition of the synergy, S, between corrosion and mechanical processes in case of tribocorrosion as:

$$W = C_0 + M_0 + S \tag{7}$$

In which:

$$S = C_M + M_C \tag{8}$$

The term *S* defined as such reflects the fact that the material mass loss in a corrosive environment cannot be predicted simply by the sum of the mass loss due to corrosion in the environment in absence of any mechanical interaction, and the material loss due to wear recorded under similar testing conditions but in an non-corrosive environment. There is a synergy between these two processes. The formalism of tribocorrosion originally proposed (Watson et al., 1995) has surely an educational value since it allows a diagnostic on the "origin of evil" under the given set of experimental conditions. The wear M_0 is by some authors measured in a test under cathodic polarization in either dry air, de-ionized water or in the presence of corrosion inhibitors (Smith, 1985; Stemp et al, 2003; Takadoum, 1996). There is still some controversy about the validity of such procedures. In practice, the results often depend on the method used which limits the overall benefit of such a decoupling. Moreover, the concepts used do not have a physical meaning, and the synergies between wear and corrosion cannot really be simplified to a summing up. Other approaches that were developed over the past decades are briefly reviewed hereafter.

3.2 Models of oxidative wear and application in aqueous environment

3.2.1 Quinn's model of mild oxidative wear

A two-step model of mild oxidational wear for steel in air was developed (Quinn, 1992, 1994). The author observed that at sliding speeds below 5 ms^{-1} the wear debris consists only

of iron oxides and that the particle size is quite constant in the range of several micrometers. In a first step oxides grow on surface asperities as a result of local heating at contact points. When the oxide reaches a critical thickness, x_c, the mechanical stresses generated in the material become too large and a detachment of the oxide layer which reaches the critical thickness takes place on the passage of the slider. The worn volume by unit of sliding distance, w, can be written as:

$$w = \frac{x_c}{Vt_c} \cdot A_r \tag{9}$$

with A_r the real contact area, V the sliding speed, and t_c the time necessary to reach the critical oxide thickness. Quinn's model is thus a law that corresponds to the Archard's wear law with:

$$K_{Archard} = \frac{x_c}{V\ t_c} \tag{10}$$

It is possible to connect x_c and t_c through a thermally activated oxidation kinetics in air which can be considered in first instance as a parabolic function with time:

$$x(t) = \alpha \sqrt{k_0 \exp\left(-\frac{Q_{act}}{R\ T_f}\right) t} \tag{11}$$

where:

- x(t) is the oxide thickness at time t,
- Q_{act} is the activation energy of the oxidation process considered,
- k_0 is the Arrhenius constant associated with the process considered,
- T_f is the flash contact temperature at the interface between two asperities,
- R is the gas constant,
- t is time, and
- α is a constant depending on the density of the oxide and its oxygen volume fraction.

The critical thickness of the oxide, x_c, can only be obtained experimentally by characterizing the debris. The model is thus not a predictive one. Moreover as pointed out (Smith, 1985) the oxide growth laws based on mass can hardly be used under the conditions of contact characterized by a low air supply, and a poor knowledge of the real contact temperature. In practice, the use of oxidation constants leads to wear rates that are several orders of magnitude different from the experimentally verified ones.

3.2.2 Model of Lemaire and Le Calvar

In conclusion, the Quinn's model can not be easily adapted to analyse the depassivation - repassivation process determining the wear laws observed in tribocorrosion conditions. However, the main idea of this model, namely that wear proceeds by a succession of growth and delamination of an oxide layer, can be retained. It was at the origin of the tribocorrosion model presented to explain the the wear of a cobalt-based alloy coating applied on the

gripper latch arms of the control rods command mechanisms in PWR (Lemaire & Le Calvar, 2000). In this model, the wear law is given by the following expression:

$$W = W_0 \, N \left(\frac{t}{t_0} \right)^{(1-n)} \qquad (12)$$

Where W is the total worn volume, W_0 a constant, and N the number of sliding steps applied to the alloy surface inducing removal of the passive film. t is the mean time interval between two successive sliding steps, and t_0 is a characteristic repassivation time constant. n is a positive exponent whose value was found experimentally close to 0.65 for the cobalt-based alloy coating. The authors explain the wear law expressed by equation (12) by the evolution of the repassivation current Ip given by expression (2). This model implies that the growth of the oxide film between two sliding steps is proportional to $t^{(1-n)}$. The Quinn's law appears as a particular case of such a model for n = 0.5. In triborrosion studies, different values of n (between 0.6 and 0.9) where found depending on the metal, the environment and the electrochemical conditions.

3.2.3 Application to the synergy formalism

Studies in corrosive aqueous solutions (Garcia et al., 2001; Jemmely et al., 2000) are suitable to follow *in situ* the growth of passive films by electrochemical methods, and allow thus the development of more sophisticated models. In these studies performed under continuous or reciprocating sliding conditions, a modeling of currents measured at an applied potential is done. It is then assumed that a unit area of depassivated material repassivates according to a simple repassivation transient, J_a (t), which is not affected by the electrochemical conditions on the areas surrounding the rubbed area. The measured total current is then the sum of the contributions of the different surface areas. A freshly depassivated area produces a large current while a area depassivated some time before produces lower currents. In the case of a reciprocating tribometer operated at a sliding frequency, f, the steady state current I can be expressed as follows assuming that each contact event depassivates the surface:

$$I = A_a \cdot f \int_0^{1/f} j_a(t)dt + (A_t - A_a)f \int_0^{1/f} j_p(t)dt \qquad (13)$$

with A_t the total area in contact with the solution, A_a the depassivated area on the sample during one cycle, f the frequency at which the surface is depassivated, j_p the passive current density at the applied potential, and j_a (t) the transient repassivation current density of a unit area at the applied potential.

Taking into consideration the synergy formalism developed above, the components of mass loss per cycle, C_M and C_0 in Equation (4) can now be written as follows:

$$C_M = \frac{M}{nF} \cdot A_a \left(\int_0^{1/f} j_a(t)dt - \int_0^{1/f} j_p(t)dt \right) \qquad (14)$$

$$C_0 = \frac{M}{nF} A_t \int_0^{1/f} j_P(t)dt \qquad (15)$$

When the component j_p related to passive zones can be neglected, C_0 becomes zero and equation (4) expressing the mass loss by corrosion under sliding becomes then:

$$C = C_M = \frac{M}{nF} A_a \int_0^{1/f} j_a(t)dt \qquad (16)$$

The depassivated area during one cycle, A_a, can hardly be assessed. Some authors assume in first instance that it is equal to the apparent area of the sliding track. However, it is well known that the contact takes place only on a fraction of that area. An evaluation of the depassivated area from currents resulting from an electrochemical depassivation achieved by a potential jump was proposed (Garcia et al., 2001). This method also allowed them to evaluate the oxide thickness formed in between two successive depassivation events. They obtained oxide layer thicknesses in the range of a few nanometers.

Another approach was developed (Jemmely et al., 2000). The authors proposed to express the depassivated area in terms of a depassivation ratio per unit of time, R_{dep} :

$$R_{dep} = f.A_a \qquad (17)$$

with f the contact frequency. The currents can then be expressed as:

$$I = R_{dep}.Q_{rep} \qquad (18)$$

with Q_{rep} the charge density for repassivation. The rate at which an active area is generated per unit of time depends on the morphology and hardness of the surfaces in contact. A derivation of R_{dep} from the scratching of a ductile material by a hard abrasive one was proposed (Adler & Walters, 1996). That approach was taken over (Jemmely et al., 2000) and extended in more general terms (Mischler et al., 1998) in the following expression:

$$R_{dep} = K.V \frac{F_N^{\beta}}{H} \qquad (19)$$

with K an empirical constant, V the sliding velocity, F_N the applied load, H the hardness of the tested material, $\beta = 0.5$ in the case of a contact between two counterparts with a similar roughness, $\beta = 0.5$ in the case of a rough and hard body against a smooth and ductile counterpart, $\beta = 1$ in the case of a hard and smooth body against a rough and ductile counterpart, and β between 0.5 and 1 in the general case.

One empirical constant K remains in this model which approximates Archard's constant and which is related to the probability that a given contact becomes depassivated. The mass loss by corrosion under sliding, C, can thus finally be written as:

$$C = \frac{M}{nF} KV \frac{F_N^{\beta}}{H} \cdot Q_{rep}(f) \qquad (20)$$

Current measurements performed at different loads and sliding speeds for materials with different hardness, allow the validation of the general form of this law.

4. Tribocorrosion testing

4.1 Specificity of laboratory and industrial tribocorrosion tests

Similarly as in classical mechanical testing, tribocorrosion tests can be classified into two categories based on their different but complementary purposes, namely fundamental and technological tests.

Fundamental tests are implemented in research laboratories and their objective is to clearly identify and to understand under well defined testing conditions, the basic mechanisms and their synergy that govern the phenomena of tribocorrosion. These tests require the development of experimental methodologies for both the test themselves and the techniques to be used for analyzing and measuring data and other experimental outcomes. Concerning friction in particular, two types of tests can be considered:

- tests at low displacement amplitude referred to as "**fretting tests**". These tests provide information on the response of materials with respect to the solicitation (displacement amplitude, load, frequency, and environment). One can differentiate stick-slip, partial slip or gross slip contact conditions. The information collected is on the nature of the degradation, its location in the contact, the kinetics of crack initiation and crack growth, and the size and shape of the degradation products that may appear in the contact during testing, and
- tests at large displacement amplitude referred to as either "**reciprocating sliding tests**" or "**continuous sliding tests**", provide information on the nature and kinetics of the wear process in connection with the synergies resulting from the mechanical, chemical or electrochemical coupling taking place on contacting surfaces in relative motion.

These tests allow the following analyses based on *in situ* and *ex situ* measurements, like the determination of the mean and local coefficient of friction, the identification of and study of the interactions between surfaces and environment, the nature of the mechanical-chemical coupling, the electrochemical or galvanic coupling due to a heterogeneous structure, the shape and location of rubbed and non-rubbed areas, or the establishment of local wear laws and their spatial distribution on the surface in view of a modelling of wear aiming at a future predictive approach.

Technological tests are designed to reproduce at lab scale mechanical loading and/or environmental conditions corresponding to actual operating conditions, or to mimic particular conditions intending to accelerate material degradation processes. These tests are widely used to predict precisely the behaviour of mechanical devices in actual conditions of service and to improve their reliability and durability. In that respect, they are very useful tools.

The full investigation of the tribocorrosion tests requires generally the use of *in situ* tools like open circuit measurements, polarization measurements, current transients, impedance spectroscopy, and noise measurements, and *ex situ* tools like elemental surface analysis techniques, optical or electron microscopy, micro-topography, micro and nanohardness measurements texture and internal stress analyses.

4.2 Testing protocol: A multiscale analysis of tribocorrosion phenomena

A promising approach of synergy in tribocorrosion has been proposed (Diomidis et al., 2009) based on the fact that the surface state of a wear track evolves with time in a cyclic manner. That evolution is due to the repeated removal and subsequent re-growth of a passive surface film when a mechanical loading is applied. During the latency time, t_{lat}, defined as the time between two successive contacts at a given point in the sliding track, the passivation reaction tends to restore the passive film. The fraction of the sliding track surface covered by this re-grown passive film increases with t_{lat}. By controlling the frequency of such depassivation-repassivation events with respect to the time necessary for film growth, it is possible to measure the properties of the surface at different stages of activity and repassivation. For performing tests at different latency times, t_{lat}, two approaches are possible, each approach having own advantages and limitations as detailed hereafter:

- first approach in the case of **continuous sliding** tests: the latency time t_{lat} can be modified by changing the rotation period t_{rot}. Another way to obtain the same t_{lat} is to keep the sliding speed constant and increase the radius of the track. However, for practical reasons, it is not realistic to consider to multiply the radius of the track by a large factor.
- second approach in the case that the latency time is changed by performing **intermittent sliding** tests: during such tests the counterbody slides for one cycle, and then stays immobile for a certain period of time to allow a part of the passive film to re-grow. Thus, an off-time, t_{off}, is imposed at the end of each cycle. As a result, the latency time between two subsequent contact events, t_{lat}, differs from the rotation period, t_{rot}:

$$t_{lat} = t_{rot} + t_{off} \tag{21}$$

It is clear that in continuous sliding tests, Equation (21) is still valid but t_{off} is zero. Such an approach can thus result in a protocol that provides information on the evolution of the surface with testing time, and the identification of the resulting mechanisms of material loss and surface degradation (Pourbaix, 1974).

4.2.1 Selection of test conditions

In order to characterize the sensitivity of the one or more material systems to tribocorrosion, a careful selection of the test conditions has to be done prior to any testing, so as to obtain discriminating results. The following steps are of large importance in that approach:

- Selection of environmental conditions: the electrolyte should be selected in view of its known oxidative or reducing power. The test temperature can be ambient temperature or any temperature relevant for the field application it should reproduce. A decisive parameter in the selection of the electrolyte is its pH. The selection of the pH can be based on pH-potential diagrams (Pourbaix, 1974). In the case of a metallic alloy, a pH range should be selected by preference where at least one of the constituents passivates. An electrolyte that may cause localized corrosion, like pitting corrosion in particular, should be avoided,
- Parameters linked to the sliding tests need to be selected by considering the following recommendations. The normal force, F_N: the normal force should be selected so as to

avoid plastic deformation of the tested materials. The maximum Hertzian contact pressure on the test material before starting sliding should be smaller than the yield strength. Concerning the track radius, R_{tr}, it should be selected in such a way that edge effects are avoided. E.g. in the case of a disc, the track radius should be by preference about half the test sample radius. Finally the number of cycles, n, depends on the type of material tested and the test conditions. It should be selected so that the wear volume is large enough to be measured accurately, while avoiding too long test durations for practical reasons. A preliminary sliding test might be necessary to determine n. In some particular cases, the selection of the number of cycles can also be done so as to reflect the behaviour of the test material in a real life application.

4.2.2 First step in the testing protocol: Electrochemical tests on passive material without any sliding

After selecting the set of appropriate test conditions, measurements are done to collect information on the electrochemical behaviour of a material fully covered by a passive film. This is done by electrochemical tests in absence of any sliding. After immersion in the electrolyte, the open circuit potential, E_{oc}, is measured versus a reference electrode. In general, a stable value of E_{oc} is obtained after some time of immersion. From an electrochemical point of view, a stable E_{oc} is obtained when the long-term fluctuations of E_{oc} are below 1 mV min^{-1} during a minimum of 1 hour. The time necessary to reach such a stationary open circuit potential in the test electrolyte is an important characteristic of a passivating process, and is called in this protocol as the reaction time characteristic, t_{reac}. The evolution of E_{oc} from immersion time on provides useful information on the electrochemical reactivity of the tested material in the test electrolyte (see Figure 7).
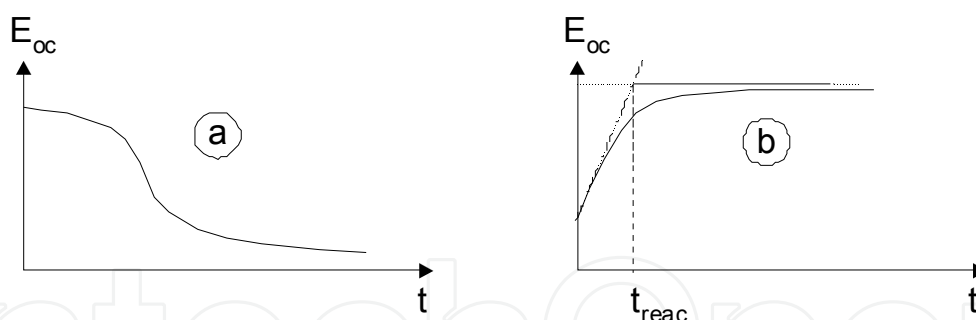
Fig. 7. Schematic representation of the evolution of E_{oc} with immersion time in the case of (a) corrosion, and (b) passivation. The graphical determination of t_{reac} in the case of passivation is shown in (b).

From this figure one can derive that when E_{oc} decreases with time, general corrosion may be suspected, and that when E_{oc} increases with time, passivation or adsorption is probably taking place. In this latter case, t_{reac} can be estimated from the evolution of E_{oc} with immersion time by drawing the tangent to the curve at the point where the slope is maximum, together with a straight line tangential to the data in the part of the curve where E_{oc} is stable. After achieving a long-term stable open circuit potential indicative of passivation, the polarization resistance of the passive material, R_p, is measured by electrochemical impedance spectroscopy. Based on R_p, the specific polarization resistance of passive material, r_{pass}, can be calculated for a test sample with a surface area, A_o, as:

$$r_{pass} = R_p . A_o \qquad (22)$$

Specific polarization resistance values for metallic materials of 10^3 Ωcm^2 or lower indicate the presence of an active sample surface, while values around 100×10^3 Ωcm^2 or higher indicate a passive sample surface. The corrosion current density of the material covered by a passive surface film, i_{pass}, is then calculated as follows:

$$i_{pass} = \frac{B}{r_{pass}} \qquad (23)$$

with B a constant. For metallic materials, B normally varies between 13 and 35 mV, depending on the nature of the material and the environment. In the protocol worked out hereafter as an example, a value of 24 mV is assumed. This passive current density, i_{pass}, is considered to correspond to the dissolution current of the material through the passive film at stationary state.

4.2.3 Second step in the testing protocol: Electrochemical tests on a fully active sliding track during sliding

The next step is the determination of the corrosion rate of the depassivated material. In order to keep continuously a part of the immersed sample surface in an active state, the passive film has to be removed by mechanical contacts. It is thus necessary to select a rotation period, t_{rot}, which is small compared to t_{reac} so that the passive film has no time to regrow in between two successive contact events. It was proposed (Diomidis et al., 2009, 2010) to take the rotation period t_{rot} equal to:

$$t_{rot} = \frac{t_{reac}}{10000} \qquad (24)$$

A first value of t_{lat1} is then taken equal to t_{rot}. It is thus assumed that during such sliding tests the whole wear track area is in an active state, so that:

$$A_{tr} = A_{act} \qquad (25)$$

Despite the fact that the width of the sliding track increases progressively due to wear during sliding tests performed against a curved counter-body, a mean sliding track area, A_{tr}, is taken for simplicity, and defined as:

$$A_{tr} = \frac{1}{2}\left(A_{tr\,max} + A_{tr\,min}\right) \qquad (26)$$

with $A_{tr\,max}$ the maximum value measured at the end of the test, and $A_{tr\,min}$ the minimum value at the end of the first cycle. $A_{tr\,min}$ is calculated by multiplying the length of the wear track, L, by the diameter of the Hertzian static contact area, e:

$$e = 2\left(\frac{3\,F_N\,R}{4\,E}\right)^{1/3} \qquad (27)$$

with F_N the applied normal load, R the radius of the tip of the curved counter-body, and E the equivalent elastic modulus given by:

$$\frac{1}{E} = \frac{1 - \nu_1^2}{E_1} + \frac{1 - \nu_2^2}{E_2} \qquad (28)$$

with ν_1 and ν_2 the Poisson's ratios, and E_1 and E_2 the elastic moduli of the test sample and counterbody respectively.

Sliding is initiated at the time a stable E_{oc} is achieved. That E_{oc} recorded during sliding is a mixed potential resulting from the galvanic coupling of material inside (A_{tr}) and outside ($A_o - A_{tr}$) the sliding track. It is assumed that the kinetics of the redox reactions taking place on each of these areas, do not vary with the real potential of the sliding track. In other words, the ohmic drop effect is considered to be negligible in the galvanic coupling between the sliding track and the surrounding area. Electrochemical impedance spectroscopy measurements are performed during sliding to obtain the polarization resistance, R_{ps}, of the sample surface. Similarly to E_{oc}, R_{ps} may be considered as the combination of two polarization resistances, namely R_{act} related to the active area A_{act} which is equal in this case to the wear track, and R_{pass} which corresponds to the surrounding unworn area, ($A_o - A_{tr}$):

$$\frac{1}{R_{ps}} = \frac{1}{R_{act}} + \frac{1}{R_{pass}} \qquad (29)$$

where

$$R_{act} = \frac{r_{act}}{A_{tr}} \qquad (30)$$

and

$$R_{pass} = \frac{r_{pass}}{A_0 - A_{tr}} \qquad (31)$$

It is then possible to calculate the specific polarization resistance of the active surface, r_{act}, as:

$$r_{act} = \frac{A_{tr} \, R_{ps} \, r_{pass}}{r_{pass} - R_{ps}(A_0 - A_{tr})} \qquad (32)$$

The corrosion current density of the active material, i_{act}, can now be obtained by substituting r_{pass} with r_{act} in Equation (23):

$$i_{act} = \frac{B}{r_{act}} \qquad (33)$$

It can be noted that, the specific resistance of the active bare material in the sliding track, r_{act}, is generally several orders of magnitude lower than the specific resistance of the material covered with a passive film, r_{pass}, outside of the sliding track. Therefore, if A_{tr} is not too small a fraction of the total area A_0 of the sample, the resistance R_{act} related to the sliding

track is small compared to the resistance R_{pass} of the area of the sample remained in passive state, outside of the sliding track: if $R_{act} \ll R_{pass}$, according to equation (29), the measured resistance R_{ps} gives then straight an approximate value of R_{act}.

4.2.4 Third step in the testing protocol: Electrochemical tests on a partially active sliding track during sliding

In the preceding steps, two extreme cases were characterized, namely on the passive material and on the active one repectively. Under tribocorrosion conditions at high latency time, the surface of the material undergoes sequential events of depassivation and repassivation in-between successive contacts. This means that a part of the surface at any given time repassivates progressively. The latency time is then selected so that the regrowth of a surface film between two successive contact events is not anymore negligible as it was the case under sliding at low latency time. To achieve partially active sliding tracks, the latency times can be selected as $t_{lat2} = t_{reac}/1000$ and $t_{lat3} = t_{reac}/100$ (Diomidis et al., 2009). As a result of the increase of the latency time in this step, the wear track can now be assumed to consist of two distinct zones (Diomidis et al., 2010), namely:

- a fraction of the sliding track from which the initial passive film has been removed during sliding. In this area, the test material may be either bare, or covered by a reaction layer different from the initial passive film. This area is named the active area, $A_{act.}$, and
- the remaining sliding track area covered by a surface film that is in the same state as the surface before sliding. This film is either not removed by the counterbody during sliding, or it had the time to restore in its initial state. This area is referred to as the repassivated area, A_{repass} with:

$$A_{tr} = A_{act} + A_{repass} \qquad (34)$$

It must be stressed that under continuous sliding, these active and repassivated areas remain constant because of stationary electrochemical state conditions. Under intermittent sliding, these active and repassivated areas on the sliding track evolve with time between two successive contact events since a gradual increase of the coverage of the repassivated area takes place within the ''off period''. By hypothesis, in both cases, the fraction of the sliding track surface covered by the passive film, A_{repass}/A_{tr}, is assumed to be constant and given by the ratio t_{lat}/t_{reac}:

$$\frac{A_{repass}}{A_{tr}} = \frac{t_{lat}}{t_{reac}} \qquad (35)$$

and:

$$\frac{A_{act}}{A_{tr}} = 1 - \frac{t_{lat}}{t_{reac}} \qquad (36)$$

At the latency times $t_{lat2} = 0.001\ t_{reac}$ and $t_{lat3} = 0.01\ t_{reac}$, the relationship between repassivated and total wear track area are respectively $A_{repass\ 2} = 0.001 A_{tr}$ and $A_{repass\ 3} = 0.01\ A_{tr}$, and thus the active wear track areas are $A_{act\ 2} = 0.999\ A_{tr}$ and $A_{act\ 3} = 0.99\ A_{tr}$.

4.3 Analysis and interpretation of sliding test results

The total wear W_{tr} in a wear track of area A_{tr} can be expressed as a sum of components related to both types of areas present on the track, the area A_{act} in active state, and the area A_{repass} in re-passivated state:

$$W_{tr} = W^c_{act} + W^m_{act} + W^c_{repass} + W^m_{repass} \tag{37}$$

with :

- W_{tr} material loss in wear track,
- W^c_{act} material loss due to corrosion of active material in wear track,
- W^m_{act} material loss due to mechanical wear of active material in wear track,
- W^c_{repass} material loss by corrosion of repassivated material in wear track, and
- W^m_{repass} material loss due to mechanical wear of repassivated material in the wear track.

In order to assess the values of these different components and to compare them to determine the characteristics of the wear mechanism, the following analyses have to be performed:

- experimental determination of the mass losses due to corrosion and mechanical wear of active material during sliding tests performed at low latency times,
- experimental determination of the mass losses due to corrosion and mechanical wear of active material during sliding tests performed at large latency times. In this case one must differentiate between continuous and intermittent sliding tests,
- experimental determination of the mass losses due to corrosion and mechanical wear of repassivated material during sliding tests performed at large latency times since they allow the study of the periodic removal and re-growth of a passive surface film,

Detailed information on the analysis and related interpretation of sliding tests can be found in a Handbook on Tribocorrosion (Celis & Ponthiaux, 2011).

5. Conclusions

Tribocorrosion is the degradation of material surfaces by the combined action of corrosion, electrochemical passivation, and external mechanical interactions. It is essentially a surface related process, but some events like hydrogen evolution and absorption by the material, can modify the mechanical properties of the sub-surfaces on materials. Under conditions where tribocorrosion is active, the material loss depends in a complex way on many parameters like the tribological conditions in the contact, the composition of the environment, the temperature, the flow rate, the pH and eventually the applied potential. By analogy it is possible to extend this concept when, in the process previously described, a chemical or physical adsorption of inhibiting species strengthens or replaces the electrochemical passivation process. The successive repetition of some of these processes can lead to a possible synergism between mechanical stress and the effect of the environment what results in a damage of surfaces and systems through an accelerated loss of functionality.

Electrochemical methods used for corrosion studies are of interest in tribocorrosion since they allow the *in situ* monitoring and analysis of the interactions between surfaces and their

environment as well as changes induced by a mechanical action like sliding or impact. In combination with conventional tribological measurements, they allow to understand the evolution of the surface state in a time space. The choice of methods to be used depends on the type of mechanical action. The data interpretations must be adapted to the heterogeneous state of surfaces undergoing a mechanical interaction, and also to the contact conditions.

Taking into account the surface state heterogeneity that results from successive mechanical and corrosive interactions, the development of an analysis of local phenomena on surfaces is needed to predict the impact of varying environmental conditions, tribological, and even geometrical ones on the operating behavior of a tribological system. Besides the methods already mentioned above, *ex situ* techniques to characterize surfaces, like the determination of residual stresses, micro-and nano-hardness, topography by 3D profilometry, chemical and structural micro-analysis of surfaces, microscopy at different length scales, must be implemented to acquire the spatial response of materials subjected to combined corrosion and mechanical loadings.

6. References

Adler T.A. & Walters R.P. (1996). Corrosion and wear of 304 stainless steel using a scratch test. *Corrosion science,* Vol 33, No. 12, pp. (1855-1876), ISSN 0010-938X.

Bom Soon Lee, Han Sub Chung, Ki-Tae Kim, Ford F.P. & Andersen P.L. (1999). Remaining life prediction methods using operating data and knowledge on mechanisms. *Nuclear Engineering and Design*, Vol. 191, No. 2, pp. (157-165), ISSN 0029-5493.

Boutard D., Wenger F., Ponthiaux P., & Galland J. (1985). Incidence de méthodes expérimentales diverses sur les diagrammes d'impédance électrochimique d'un alliage fer-31% nickel en cours de corrosion. *Proceedings of 8th European Corrosion Congress*, ISBN 2-88074-228-5, Nice (France), November 1985.

Carton J. F., Vannes A. B. & Vincent L. (1995). Basis of a coating choice methodology in fretting. *Wear*, Vol 185, No.5, 1995, pp. (47-57), ISSN 0043-1648.

Celis J.P. & Ponthiaux P. editors. (2011), *Testing tribocorrosion of passivating materials supporting research and industrial innovation: Handbook"*, EFC Green Book N° 62, Maney, ISBN 978 1 907975 20 2, Leeds (UK).

Cottis R. A. & Loto C. A. (1990). Electrochemical noise generation during SCC of a high-strength carbon steel. *Corrosion*, Vol. 46, No.1, pp. (12-19), ISSN 0010-9312.

Déforge D., Huet F., Nogueira R.P., Ponthiaux P., and Wenger F. (2006). Electrochemical noise analysis of tribocorrosion processes under steady-state friction regime. *Corrosion*, Vol. 62, No 6, pp. (514-521), ISSN 0010-9312.

Diomidis N., Celis J.-P., Ponthiaux P. & Wenger F. (2009). A methodology for the assessment of the tribocorrosion of passivating metallic materials. *Lubrication Science*, Vol. 21, No 2, pp. (53-67), ISSN 0954-0075.

Diomidis N., Celis J.P., Ponthiaux P. & Wenger F. (2010). Tribocorrosion of stainless steel in sulfuric acid: Identification of corrosion–wear components and effect of contact area. *Wear*, Vol. 269, No 1-2, pp. (93-103), ISSN 0043-1648.

Garcia, I., Drees, D. & Celis, J.-P. (2001). Corrosion-wear of passivating materials in sliding contacts based on a concept of active wear track area. *Wear*, Vol. 249, No *5-6,* pp. (452-460), ISSN 0043-1648.

Godet M., Berthier Y., Lancaster J. & Vincent L. (1991). Wear modelling : using fundamental understanding or practical experience ?, *Wear*, Vol. 149, No 1-2, pp. (325-340), ISSN 0043-1648.

Jemmely, P., Mischler, S. & Landolt, D. (2000). Electrochemical modelling of passivation phenomena in tribocorrosion. *Wear*, Vol. 237, No. 1, pp. (63-76), ISSN 0043-1648.

Law C. G., & Newman J. (1979). A model for the anodic dissolution of iron in sulfuric acid. *Journal of the Electrochemical. Society.*, Vol. 126, No.12, pp. (2150-2155), ISSN 0043-1648.

Lemaire E. & Le Calvar M. (2000). Evidence of tribocorrosion wear in pressurized water reactors. *Wear*, Vol. 249, No. 5-6, pp. (1-7), ISSN 0043-1648.

Lillard R. S., Kruger J., Tait W. S. & Moran P. J. (1995). Using local electrochemical impedance spectroscopy to examine coating failure. *Corrosion*, Vol. 51, No. 4, pp. 251-259 ISSN 0010-9312.

Lim, S.C. & Ashby, M.F. (1987). Wear-mechanism maps. *Acta Metallurgica*, Vol. 35, No. 1, pp. (1-24), ISSN 1359-6454.

Mischler S., Ayrault S., Debaud S., Jemmely Ph., Rosset E. & Landolt D. (1997). Aspects physico-chimiques de la tribocorrosion. *Matériaux et Techniques*, Vol. HS, No. July, pp. (5-10), ISSN 0032-6895.

Mischler, S., Debaud, S. & Landolt, D. (1998). Wear-accelerated corrosion of passive metals in tribocorrosion systems. *Journal of the Electrochemical. Society.*, Vol. 145, No. 3, pp. (750-758), ISSN 0043-1648.

Oltra R. & Keddam M. (1990). Application of E.I.S. to localized corrosion. *Electrochimica Acta*, Vol. 35, No. 10, pp. (1619-1629), ISSN 0013-4686.

Oltra R., Gabrielli G., Huet F. & Keddam M. (1986). Electrochemical investigation of locally depassivated iron. A comparison of various techniques. *Electrochimica Acta*, Vol. 31, No. 12, pp. (1501-1511), ISSN 0013-4686.

Ponthiaux P., Wenger F. & Galland J. (1995). Study of the anodic current-voltage curve of an iron-nickel alloy in normal sulfuric acid. *Journal of the Electrochemical. Society.*, Vol. 142, No. 7, pp. (2204-2210), ISSN 0043-1648.

Ponthiaux P., Wenger F., Galland J., Lederer G. & Celati N. (1997). Utilisation du bruit électrochimique pour déterminer la surface dépassivée par frottement. Cas d'un acier Z2 CND 17-13 en milieu chloruré (NaCl 3%), *Matériaux et Techniques*, Vol. HS, No. July, pp. (43-46), ISSN 0032-6895.

Ponthiaux P., Wenger F., Galland J., Kubecka P. & Hyspecka L. (1999). Effets combinés du frottement et de la corrosion dans le cas d'un alliage fer-nickel en milieu sulfurique. *Matériaux et Techniques*, Vol. HS, No. December, pp. (11-15), ISSN 0032-6895.

Pourbaix M. (1974), *Atlas of Electrochemical Equilibria in Aqueous Solutions*, National Association of Corrosion Engineers, ISBN 0915567989, Houston (USA).

Quinn, T.F.J. (1992). Oxidational wear modelling: part I. *Wear*, Vol. 153, No. 1, pp. (179-200), ISSN 0043-1648.

Quinn, T.F.J. (1994). Oxidational wear modelling: part II. The general theory of oxidational wear. *Wear*, Vol. 175, No. 1-2, pp. (199-208), ISSN 0043-1648.

Rosset E. (1999). Tribologie Systémique. *Oberflächen-Polysurface*, Vol. 1, pp. (7-9), ISSN 1422-3511.

Smith A.F. (1985). Sliding wear of AISI 316 stainless steel in air, 20 - 500°C. *Tribology International*, Vol. 18, No. 1, pp. (35–43), ISSN 0301-679X.

Stemp M., Mischler S. & Landolt D. (2003). The effect of mechanical and electrochemical parameters on the tribocorrosion rate of stainless steel in sulfuric acid. *Wear*, Vol. 255, No.1-6, pp. (466–475), ISSN 0043-1648.

Takadoum J. (1996). The influence of potential on the tribocorrosion of nickel and iron in sulfuric acid solution. *Corrosion Science*, Vol. 38, No. 4, pp. (643–654), ISSN 0010-938X.

Tiedemann W. H., Newman J. & Bennion D. N. (1973). The errors in measurements of electrode kinetics caused by nonuniform ohmic-potential drop to a disk electrode. *Journal of the Electrochemical. Society.*, Vol. 120, No. 2, , pp. (256-258), ISSN 0043-1648.

Uruchurtu J. C. & Dawson J. L. (1987). Noise analysis of pure aluminium under different pitting conditions. *Corrosion*, Vol. 43, No. 1, pp. (19-25), ISSN 0010-9312.

Watson, S.W., Friedersdorf, F.J., Madsen, B.W. & Cramer, S.D. (1995). Methods of measuring wear-corrosion synergism. *Wear*, Vol. 181-183, No. 2, pp. 476-484, ISSN 0043-1648.

Zhang J., Wenger F. & Galland J. (1987). Contrôle de l'état local de corrosion de structures métalliques de grandes dimensions par les mesures d'impédance électrochimiques. *Comptes Rendus de l'Académie des Sciences, Paris,* Série 2, Vol. 304, No. 14, pp. (797-800), ISSN 12518069.

Corrosion Resistance

Edited by Dr Shih

ISBN 978-953-51-0467-4

Hard cover, 472 pages

Publisher InTech

Published online 30, March, 2012

Published in print edition March, 2012

The book has covered the state-of-the-art technologies, development, and research progress of corrosion studies in a wide range of research and application fields. The authors have contributed their chapters on corrosion characterization and corrosion resistance. The applications of corrosion resistance materials will also bring great values to reader's work at different fields. In addition to traditional corrosion study, the book also contains chapters dealing with energy, fuel cell, daily life materials, corrosion study in green materials, and in semiconductor industry.

INTECH

open science | open minds